LETTER

doi:10.1038/nature21045

Ruthenium isotopic evidence for an inner Solar System origin of the late veneer

Mario Fischer-Gödde[1] & Thorsten Kleine[1]

The excess of highly siderophile elements in the Earth's mantle is thought to reflect the addition of primitive meteoritic material after core formation ceased[1–4]. This 'late veneer' either comprises material remaining in the terrestrial planet region after the main stages of the Earth's accretion[5,6], or derives from more distant asteroidal[7] or cometary[8] sources. Distinguishing between these disparate origins is important because a late veneer consisting of carbonaceous chondrite-like asteroids[7] or comets[8] could be the principal source of the Earth's volatiles and water. Until now, however, a 'genetic' link between the late veneer and such volatile-rich materials has not been established or ruled out. Such genetic links can be determined using ruthenium (Ru) isotopes, because the Ru in the Earth's mantle predominantly derives from the late veneer[9], and because meteorites exhibit Ru isotope variations arising from the heterogeneous distribution of stellar-derived dust[10,11]. Although Ru isotopic data and the correlation of Ru and molybdenum (Mo) isotope anomalies in meteorites were previously used to argue that the late veneer derives from the same type of inner Solar System material as do Earth's main building blocks[6], the Ru isotopic composition of carbonaceous chondrites has not been determined sufficiently well to rule them out as a source of the late veneer. Here we show that all chondrites, including carbonaceous chondrites, have Ru isotopic compositions distinct from that of the Earth's mantle. The Ru isotope anomalies increase from enstatite to ordinary to carbonaceous chondrites, demonstrating that material formed at greater heliocentric distance contains larger Ru isotope anomalies. Therefore, these data refute an outer Solar System origin for the late veneer and imply that the late veneer was not the primary source of volatiles and water on the Earth.

The major period of the Earth's accretion probably ended with a giant impact from a body greater than 5% of the Earth's mass, leading to the formation of the Moon[12,13]. However, after this event, the Earth continued to accrete material, amounting to about 0.5% of its present mass[14]. Evidence for this late accretion comes primarily from the abundances of the highly siderophile elements in the Earth's primitive mantle[9], which are higher than expected for metal–silicate partitioning during core formation[3]. These are, therefore, best explained by the addition of primitive meteoritic material (the 'late veneer') after the Moon-forming impact and the cessation of core formation[1–4]. Constraining the origin, nature and chemical composition of the late veneer is important not only for providing fundamental insights into the dynamics of terrestrial planet formation, but also for constraining the origin of the Earth's water and volatile elements.

Although the total mass added during late accretion is small, a carbonaceous chondrite-like late veneer may nevertheless be the dominant source of the Earth's water[7]. This observation has led to the idea that the Earth accreted 'dry' and that water and highly volatile elements were added only later, after the Moon-forming impact, by the addition of volatile-rich bodies from the outer Solar System[8]. However, although the most plausible sources of the Earth's water are bodies from the outer Solar System[15], it is unclear whether such bodies were added during late accretion or during the main stages of the Earth's growth[8,16–18].

Distinguishing between these two possibilities requires information both on the chemical composition of the late veneer and on potential genetic links between the late veneer, meteorites and the Earth's main building blocks. However, until now it has not been possible to establish such links unequivocally. For instance, osmium (Os) isotope systematics, reflecting the long-term ratio of rhenium (Re) to Os, have been used to argue for a late veneer made up of ordinary or enstatite chondrites[14,19], but have also been explained by a late veneer consisting of a mixture of carbonaceous chondrites and iron meteorites[20]. Likewise, selenium (Se)–tellurium (Te)–sulphur (S) elemental systematics suggest a carbonaceous-chondrite-like late veneer[7], but the viability of using the abundances of these elements in the Earth's mantle to identify the source of the late veneer has been questioned[21]. These examples illustrate that determining the chemical composition of the Earth's mantle with sufficient precision to discriminate between different chondrite groups as potential sources of the late veneer is problematic.

More powerful constraints on the genetic heritage of the late veneer can be obtained from nucleosynthetic isotope anomalies. These anomalies arise through the heterogeneous distribution of presolar matter, and so only samples having the same nucleosynthetic isotope composition (that is, containing the same specific mixture of presolar components) can be genetically linked. Thus, the genetic characteristics of the late veneer can be examined via the absence or presence of nucleosynthetic isotope anomalies. Ru isotopes are ideally suited for this task, because (1) as a highly siderophile element, almost all the Ru in the Earth's mantle should derive from the late veneer[3,9,14], and (2) Ru isotopic compositions in meteorites vary owing to the heterogeneous distribution of a presolar component enriched in *s*-process matter[10,11]. Prior studies have shown that the Ru isotopic composition of the Earth's mantle is most similar to enstatite chondrites and distinct from ordinary chondrites as well as most iron meteorites[10,11]. Moreover, on the basis of correlated Ru and Mo isotope anomalies in meteorites it was argued that the late veneer (which determines the Ru isotopic composition of the Earth's mantle) derives from the same type of material as the main building blocks of the Earth (which determine the Mo isotopic composition of the Earth's mantle)[6].

Although these data suggest that the late veneer derives from inner Solar System material, so far Ru isotopic data for carbonaceous chondrites are very limited and only two samples have been analysed[10,11]. Moreover, for these samples disparate results have been reported[10,11], including both excesses and deficits in Ru produced in the slow neutron capture process (*s*-process) of stellar nucleosynthesis. Thus, in general, the Ru isotopic characteristics of carbonaceous chondrites are poorly defined. Moreover, as the two carbonaceous chondrites so far analysed do not seem to plot on the Mo–Ru correlation defined by other meteorites, any genetic link of the carbonaceous chondrites to both the main building material of the Earth and the late veneer remains uncertain[11]. Therefore, the limited Ru isotope data set for carbonaceous chondrites precludes a reliable assessment of whether such material is a viable source of the late veneer.

[1]Institut für Planetologie, University of Münster, Wilhelm-Klemm-Strasse 10, 48149 Münster, Germany.

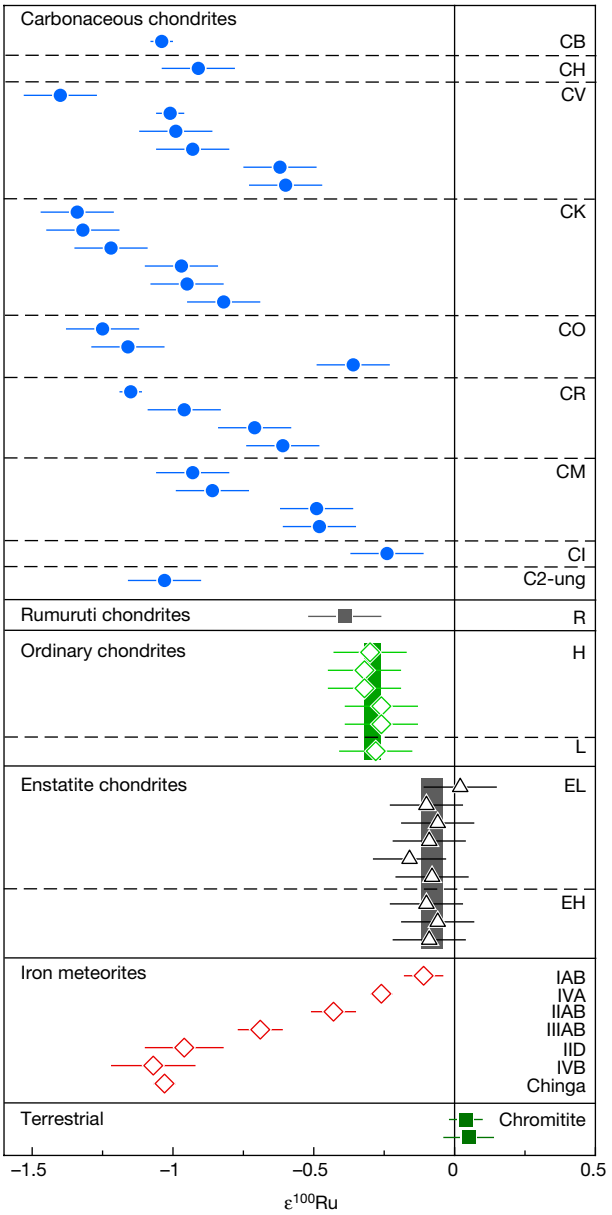

Figure 1 | ϵ^{100}Ru data for chondrites, iron meteorites and terrestrial chromitites. See Extended Data Table 1 and source data for Fig. 2. Shown are individual data points for all analysed samples and the average neutron-capture-corrected ϵ^{100}Ru for IAB iron meteorites (see Extended Data Table 2). Data for other iron meteorite groups[11] are shown for comparison. The uncertainties shown for individual data points reflect the external uncertainty of the method (2 s.d. for samples measured $n < 4$ times) or 95% confidence intervals of replicates of a sample (if $n \geq 4$). The shaded areas represent the mean values for ordinary and enstatite chondrites with their 95% confidence interval uncertainties.

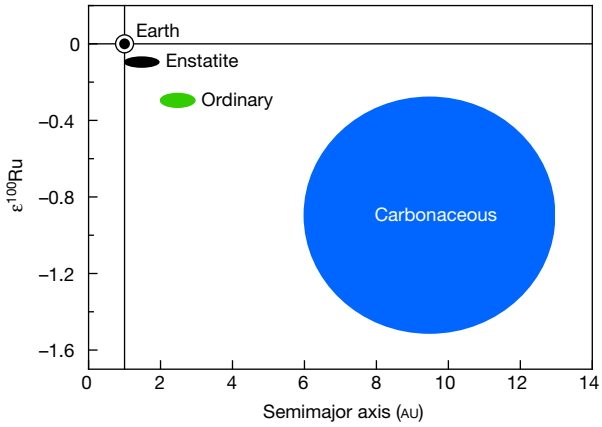

Figure 2 | The magnitude of ϵ^{100}Ru anomalies increases with increasing distance (in astronomical units, au) from the Sun. More reduced materials like enstatite and ordinary chondrites have less negative ϵ^{100}Ru compared to more oxidized and volatile-rich materials such as carbonaceous chondrites that formed at greater heliocentric distance. Shown are mean ϵ^{100}Ru values for different chondrite classes: enstatite chondrites ($\epsilon^{100}\text{Ru} = -0.08 \pm 0.04$, 95% confidence interval); ordinary chondrites ($\epsilon^{100}\text{Ru} = -0.29 \pm 0.03$, 95% confidence interval); carbonaceous chondrites ($\epsilon^{100}\text{Ru} = -0.9 \pm 0.6$, 2 s.d.). Semimajor axes for the different chondrite classes are based on the Grand Tack model[18,30,31]. (See source data for Fig. 2.)

To address this issue, we obtained Ru isotopic data for a comprehensive set of chondrites, including carbonaceous chondrites from eight different groups, the primitive ungrouped carbonaceous chondrite Tagish Lake, seven enstatite chondrites, one ordinary and one Rumuruti chondrite (Extended Data Table 1). We also analysed four non-magmatic iron meteorites (Extended Data Table 2), because prior studies reported terrestrial Ru isotopic compositions for these samples[10,11], suggesting that they may derive from the same population of bodies as the late veneer. The primitive chondrites were digested by alkaline fusion for complete dissolution of all presolar components[11], as more common acid and Carius tube digestion techniques cannot fully dissolve some presolar components such as silicon carbide (SiC)[22,23]. To assess the Ru isotopic composition of the Earth's mantle, we analysed two terrestrial chromitites (Extended Data Table 1). Isotopically, these were indistinguishable from the Ru solution standard, suggesting that their Ru isotope composition is representative for the Earth's mantle. Compared to the chromitites and the Ru solution standard, all chondrite groups and the non-magmatic irons exhibit resolved nucleosynthetic Ru isotope anomalies reflecting the heterogeneous distribution of an *s*-process carrier (Fig. 1, Extended Data Fig. 1, Extended Data Tables 1 and 2). The Ru isotope anomalies are most pronounced for ϵ^{100}Ru (the parts per 10,000 deviation of the ^{100}Ru/^{101}Ru ratio from the terrestrial standard value), where carbonaceous chondrites (including Tagish Lake) display the largest (ϵ^{100}Ru up to about −1.4) anomalies, while enstatite chondrites (average $\epsilon^{100}\text{Ru} = -0.08 \pm 0.04$, 95% confidence, $n = 9$) and non-magmatic irons (average $\epsilon^{100}\text{Ru} = -0.11 \pm 0.07$, 95% confidence, $n = 4$) have the smallest resolved anomalies. The carbonaceous chondrites show large within-group variations with ϵ^{100}Ru values ranging from −0.2 to −1.4 (Fig. 1), most probably resulting from nebular or parent body processes acting on the presolar components of these meteorites, leading to isotopic variations at the sampling scale. Nevertheless, all analysed meteorites display negative ϵ^{100}Ru values, indicating that compared to the Earth's mantle, they are all deficient in *s*-process Ru (Fig. 1).

This omnipresent deficit indicates that a depletion in *s*-process Ru relative to the Earth's mantle is a general characteristic of material from the present-day asteroid belt; otherwise, there is no reason why only material with *s*-process Ru deficits should be delivered to the Earth as meteorites. Moreover, the magnitude of the ϵ^{100}Ru isotope anomalies decreases in the order carbonaceous > ordinary > enstatite chondrites, indicating that there is a heliocentric zoning of nucleosynthetic Ru isotope anomalies (Fig. 2). This is consistent with the large Ru isotopic anomaly ($\epsilon^{100}\text{Ru} = -1.03 \pm 0.13$) of Tagish Lake, because this meteorite probably derives from a volatile-rich body located beyond the main asteroid belt[24,25]. These data, therefore, suggest that material from the outer Solar System, such as comets, also have a strong deficit in *s*-process Ru, similar to or even larger than observed for carbonaceous chondrites.

If, as commonly assumed, virtually all Ru in the Earth's mantle derives from the late veneer, then our data rule out that the late veneer was comprised of meteorites or other asteroidal bodies. This is because no single group of chondrites nor any combination of chondrites and iron meteorites would reproduce the Ru isotopic composition of the Earth's

mantle. Our data are also inconsistent with a cometary origin of the late veneer, as proposed in some dynamic models[8], because, as argued above, bodies from the outer Solar System are probably characterized by a large deficit in *s*-process Ru. Combined, these data therefore suggest that the late veneer derives from bodies in the inner Solar System.

If, as recently proposed, only about 60% of the Ru in the Earth's mantle was added by the late veneer[26], then a late veneer having a deficit in *s*-process Ru, as observed for meteorites, would have to be balanced by an *s*-process-enriched composition of the Ru in the Earth's pre-late veneer mantle. For instance, if the pre-late veneer mantle had a ε^{100}Ru anomaly of $+0.12 \pm 0.05$, then addition of an enstatite-chondrite-like late veneer would have resulted in $\epsilon^{100}\mathrm{Ru} \approx 0$ for the present-day mantle. Thus, if a large fraction of Ru in the silicate Earth does not derive from the late veneer, then the late veneer could consist of meteoritic material with a small deficit in *s*-process Ru, such as enstatite chondrites. However, given that most carbonaceous chondrites typically have a large *s*-process deficit of $\epsilon^{100}\mathrm{Ru} \approx -1$, a late veneer with this composition would require the Earth's pre-late-veneer mantle (that is, the mantle before the late veneer was added) to have an excess in *s*-process Ru of about the same magnitude (that is, $\epsilon^{100}\mathrm{Ru} \approx +1$). This composition for the Earth's pre-late-veneer mantle is unlikely, however, because for several elements (Ca, Ti, Ni, Cr, O) the Earth is isotopically most similar to enstatite chondrites[27]. Because these elements record the Earth's entire accretion history and, therefore, indicate that the Earth's major building blocks are, on average, isotopically similar to enstatite chondrites, any reasonable Ru isotopic composition of the pre-late-veneer mantle should also be close to that of enstatite chondrites ($\epsilon^{100}\mathrm{Ru} = -0.08 \pm 0.04$). Consequently, the Earth's pre-late-veneer mantle is unlikely to have contained a large positive ϵ^{100}Ru anomaly, as would be required by a carbonaceous chondrite-like late veneer. Thus, even if not all the Ru in the present-day Earth's mantle derives from the late veneer, the Ru isotopic data still rule out the possibility that the late veneer consisted of carbonaceous chondrites.

Although our results demonstrate that the late veneer is not comprised of carbonaceous chondrites, the abundances and isotopic compositions of hydrogen, carbon and nitrogen indicate that the Earth's volatiles probably derived from carbonaceous-chondrite-like material[28,29]. These seemingly contradictory observations can be reconciled if carbonaceous-chondrite-like objects were scattered into the inner Solar System early in the Earth's accretion, as predicted in recent dynamical models[30,31]. Such bodies would probably be characterized by a deficit in *s*-process Ru compared to the present-day Earth's mantle, but because this material was added during the main stages of accretion and core formation this Ru would have been quantitatively removed to the Earth's core and thus would not have affected the Ru isotopic composition of the Earth's mantle. Thus, our Ru isotopic data are consistent with the accretion of volatile-rich bodies from the outer Solar System during the main stages of terrestrial planet formation, but not during late accretion.

Online Content Methods, along with any additional Extended Data display items and Source Data, are available in the online version of the paper; references unique to these sections appear only in the online paper.

Received 21 March; accepted 7 December 2016.

1. Kimura, K., Lewis, R. S. & Anders, E. Distribution of gold and rhenium between nickel-iron and silicate melts—implications for abundance of siderophile elements on Earth and Moon. *Geochim. Cosmochim. Acta* **38,** 683–701 (1974).
2. Chou, C. L. Fractionation of siderophile elements in the Earth's upper mantle. *Proc. Lunar Planet. Sci. Conf.* **IX,** 219–230 (1978).
3. Brenan, J. M. & McDonough, W. F. Core formation and metal-silicate fractionation of osmium and iridium from gold. *Nat. Geosci.* **2,** 798–801 (2009).
4. Walker, R. J. Highly siderophile elements in the Earth, Moon and Mars: update and implications for planetary accretion and differentiation. *Chem Erde-Geochem.* **69,** 101–125 (2009).
5. Bottke, W. F., Walker, R. J., Day, J. M. D., Nesvorny, D. & Elkins-Tanton, L. Stochastic late accretion to Earth, the Moon, and Mars. *Science* **330,** 1527–1530 (2010).
6. Dauphas, N., Davis, A. M., Marty, B. & Reisberg, L. The cosmic molybdenum-ruthenium isotope correlation. *Earth Planet. Sci. Lett.* **226,** 465–475 (2004).
7. Wang, Z. & Becker, H. Ratios of S, Se and Te in the silicate Earth require a volatile-rich late veneer. *Nature* **499,** 328–331 (2013).
8. Albarède, F. Volatile accretion history of the terrestrial planets and dynamic implications. *Nature* **461,** 1227–1233 (2009).
9. Becker, H. *et al.* Highly siderophile element composition of the Earth's primitive upper mantle: Constraints from new data on peridotite massifs and xenoliths. *Geochim. Cosmochim. Acta* **70,** 4528–4550 (2006).
10. Chen, J. H., Papanastassiou, D. A. & Wasserburg, G. J. Ruthenium endemic isotope effects in chondrites and differentiated meteorites. *Geochim. Cosmochim. Acta* **74,** 3851–3862 (2010).
11. Fischer-Gödde, M., Burkhardt, C., Kruijer, T. S. & Kleine, T. Ru isotope heterogeneity in the solar protoplanetary disk. *Geochim. Cosmochim. Acta* **168,** 151–171 (2015).
12. Canup, R. M. Forming a Moon with an Earth-like Composition via a giant impact. *Science* **338,** 1052–1055 (2012).
13. Cuk, M. & Stewart, S. T. Making the Moon from a fast-spinning Earth: a giant impact followed by resonant despinning. *Science* **338,** 1047–1052 (2012).
14. Walker, R. J. *et al.* In search of late-stage planetary building blocks. *Chem. Geol.* **411,** 125–142 (2015).
15. Morbidelli, A. *et al.* Source regions and timescales for the delivery of water to the Earth. *Meteorit. Planet. Sci.* **35,** 1309–1320 (2000).
16. Ballhaus, C. *et al.* The U/Pb ratio of the Earth's mantle: a signature of late volatile addition. *Earth Planet. Sci. Lett.* **362,** 237–245 (2013).
17. Wood, B. J. & Halliday, A. N. The lead isotopic age of the Earth can be explained by core formation alone. *Nature* **465,** 767–770 (2010).
18. Rubie, D. C. *et al.* Accretion and differentiation of the terrestrial planets with implications for the compositions of early-formed Solar System bodies and accretion of water. *Icarus* **248,** 89–108 (2015).
19. Meisel, T., Walker, R. J. & Morgan, J. W. The osmium isotopic composition of the Earth's primitive upper mantle. *Nature* **383,** 517–520 (1996).
20. Fischer-Gödde, M. & Becker, H. Osmium isotope and highly siderophile element constraints on ages and nature of meteoritic components in ancient lunar impact rocks. *Geochim. Cosmochim. Acta* **77,** 135–156 (2012).
21. König, S., Lorand, J.-P., Luguet, A. & Graham Pearson, D. A non-primitive origin of near-chondritic S–Se–Te ratios in mantle peridotites; implications for the Earth's late accretionary history. *Earth Planet. Sci. Lett.* **385,** 110–121 (2014).
22. Brandon, A. D., Humayun, M., Puchtel, I. S., Leya, I. & Zolensky, M. Osmium isotope evidence for an s-process carrier in primitive chondrites. *Science* **309,** 1233–1236 (2005).
23. Yokoyama, T. *et al.* Osmium isotope evidence for uniform distribution of *s*- and *r*-process components in the early solar system. *Earth Planet. Sci. Lett.* **259,** 567–580 (2007).
24. Hiroi, T., Zolensky, M. E. & Pieters, C. M. The Tagish Lake meteorite: a possible sample from a D-type asteroid. *Science* **293,** 2234–2236 (2001).
25. Brandon, A. D., Humayun, M., Puchtel, I. S. & Zolensky, M. E. Re-Os isotopic systematics and platinum group element composition of the Tagish Lake carbonaceous chondrite. *Geochim. Cosmochim. Acta* **69,** 1619–1631 (2005).
26. Rubie, D. C. *et al.* Highly siderophile elements were stripped from Earth's mantle by iron sulfide segregation. *Science* **353,** 1141–1144 (2016).
27. Dauphas, N. *et al.* Calcium-48 isotopic anomalies in bulk chondrites and achondrites: evidence for a uniform isotopic reservoir in the inner protoplanetary disk. *Earth Planet. Sci. Lett.* **407,** 96–108 (2014).
28. Alexander, C. M. O. D. *et al.* The provenances of asteroids, and their contributions to the volatile inventories of the terrestrial planets. *Science* **337,** 721–723 (2012).
29. Marty, B. The origins and concentrations of water, carbon, nitrogen and noble gases on Earth. *Earth Planet. Sci. Lett.* **313–314,** 56–66 (2012).
30. O'Brien, D. P., Walsh, K. J., Morbidelli, A., Raymond, S. N. & Mandell, A. M. Water delivery and giant impacts in the 'Grand Tack' scenario. *Icarus* **239,** 74–84 (2014).
31. Walsh, K. J., Morbidelli, A., Raymond, S. N., O'Brien, D. P. & Mandell, A. M. A low mass for Mars from Jupiter's early gas-driven migration. *Nature* **475,** 206–209 (2011).

Acknowledgements We thank the Meteorite Working Group at NASA, A. Bischoff and A. Greshake for providing the meteorite samples for this study, and K. Bermingham and B. O'Driscoll for providing the Shetland chromitite sample. We thank U. Heitmann, T. Kruijer and C. Proksche for their assistance, and A. Brandon, C. Brennecka and D. Papanastassiou for comments on the paper. This work was supported by the Deutsche Forschungsgemeinschaft (SFB-TRR 170, subproject B3-1). This is TRR 170 publication no. 11.

Author Contributions M.F.-G. prepared the samples for Ru isotope analyses and conducted the measurements. Both M.F.-G. and T.K. were involved in the interpretation of the data and the writing of the manuscript.

Author Information Reprints and permissions information is available at www.nature.com/reprints. The authors declare no competing financial interests. Readers are welcome to comment on the online version of the paper. Correspondence and requests for materials should be addressed to M.F.-G. (m.fischer-goedde@uni-muenster.de) or T.K. (thorsten.kleine@uni-muenster.de).

Reviewer Information *Nature* thanks A. Brandon and the other anonymous reviewer(s) for their contribution to the peer review of this work.

METHODS

Bulk pieces of chondrites (approximately 1–4 g) were carefully cleaned using SiC paper and ultrasonication in distilled water, and were then powdered in an agate mortar used exclusively for the preparation of meteorites. Aliquots of the chondrite powders (approximately 0.5 g) were either decomposed by alkaline fusion (chondrites with petrologic types of 1 to 4)[11] in glassy carbon containers or using reverse aqua regia inside Pyrex Carius tubes (chondrites of petrologic types 5 and 6)[11]. The chromitites were digested using both techniques. Samples of non-magmatic iron meteorites (approximately 0.5 g) were cut and surfaces were cleaned with SiC paper and ethanol. Iron meteorite samples were leached for about 15 min in 6 M HCl and then dissolved in 6 M HCl with traces of concentrated HNO_3 in PFA Teflon beakers on a hotplate. For samples digested in Carius tubes and PFA Teflon beakers, Ru was separated by cation exchange chromatography followed by micro-distillation, whereas for samples decomposed by alkaline fusion, Ru was purified using a Teflon distillation unit without prior purification by cation exchange chromatography[11]. Total procedural blanks were 43 ± 14 pg ($n = 5$, 1 s.d.) for samples processed in Carius tubes or PFA Teflon beakers and 86 ± 16 pg ($n = 4$, 1 s.d.) for samples digested by alkaline fusion. The Ru isotope measurements were performed using the ThermoScientific Neptune Plus multicollector inductively coupled plasma mass spectrometer (MC-ICPMS) in the Institut für Planetologie at the University of Münster. Samples were dissolved in 0.28 M HNO_3 and introduced into the mass spectrometer at an uptake rate of 40–50 μl min^{-1} using a Savillex C-Flow PFA nebulizer attached to a Cetac Aridus II desolvator. The measurements were typically performed with total ion beam intensities ranging from 8×10^{-11} A to 3×10^{-10} A, which were obtained for a Ru solution of about 100 parts per billion using conventional Ni H-cones. The signal was optimized to achieve oxide rates of much less than 1% (CeO/Ce). Isotopic measurements were performed in static mode and the seven stable Ru isotopes ^{96}Ru, ^{99}Ru, ^{98}Ru, ^{101}Ru, ^{102}Ru and ^{104}Ru as well as ^{97}Mo and ^{105}Pd were monitored simultaneously. Each Ru isotope analysis consisted of an on-peak baseline measurement on a solution blank (40 times 8.4 s) followed by 100 integrations of 8.4 s each of sample or standard solution and typically consumed about 90 ng Ru. Each sample analysis was bracketed by measurements of an in-house Ru solution standard (Alfa Aesar Ru). Mass bias was corrected by internal normalization to $^{99}Ru/^{101}Ru = 0.7450754$ using the exponential law. The Ru isotope data are reported as $\epsilon^{i}Ru = [(^{i}Ru/^{101}Ru)_{sample}/(^{i}Ru/^{101}Ru)_{standard} - 1] \times 10{,}000$, calculated relative to the mean value of the bracketing standard runs of each analytical session. The accuracy and precision of the Ru isotope measurements were evaluated by replicate digestions and multiple analyses of different types of terrestrial reference materials (UB-N, BCR-2, BHVO-2, NIST 129c, NIST 361), doped with 500–2,000 ng Ru from the same Alfa Aesar solution standard used to bracket the Ru isotope measurements of samples[11]. Doped samples were processed through the whole purification procedure and yielded ϵ^{i}Ru values of approximately 0, demonstrating that our Ru isotopic data are accurate. The external reproducibility (2 s.d.) of the Ru isotope analyses obtained for all processed reference samples (including 84 individual measurements from 18 digestions of 5 different reference samples) is ± 0.45 ϵ^{96}Ru, ± 0.52 ϵ^{98}Ru, ± 0.13 ϵ^{100}Ru, ± 0.15 ϵ^{102}Ru, and ± 0.31 ϵ^{104}Ru (ref. 11). To test our analytical method further and to assess the Ru isotope composition of the Earth's mantle, we have analysed chromitite samples from the Shetland Ophiolite Complex in Scotland (C3) and the Bushveld Complex in South Africa (UG2); both yielded the same Ru isotopic composition as the Ru solution standard within uncertainty.

Data availability. The data that support the findings of this study are available from the EarthChem library (http://dx.doi.org/10.1594/IEDA/100622).

32. Savina, M. R. *et al.* Extinct technetium in silicon carbide stardust grains: implications for stellar nucleosynthesis. *Science* **303,** 649–652 (2004).
33. Bisterzo, S., Gallino, R., Straniero, O., Cristallo, S. & Käppeler, F. The *s*-process in low-metallicity stars—II. Interpretation of high-resolution spectroscopic observations with asymptotic giant branch models. *Mon. Not. R. Astron. Soc.* **418,** 284–319 (2011).
34. Kruijer, T. S. *et al.* Neutron capture on Pt isotopes in iron meteorites and the Hf-W chronology of core formation in planetesimals. *Earth Planet. Sci. Lett.* **361,** 162–172 (2013).

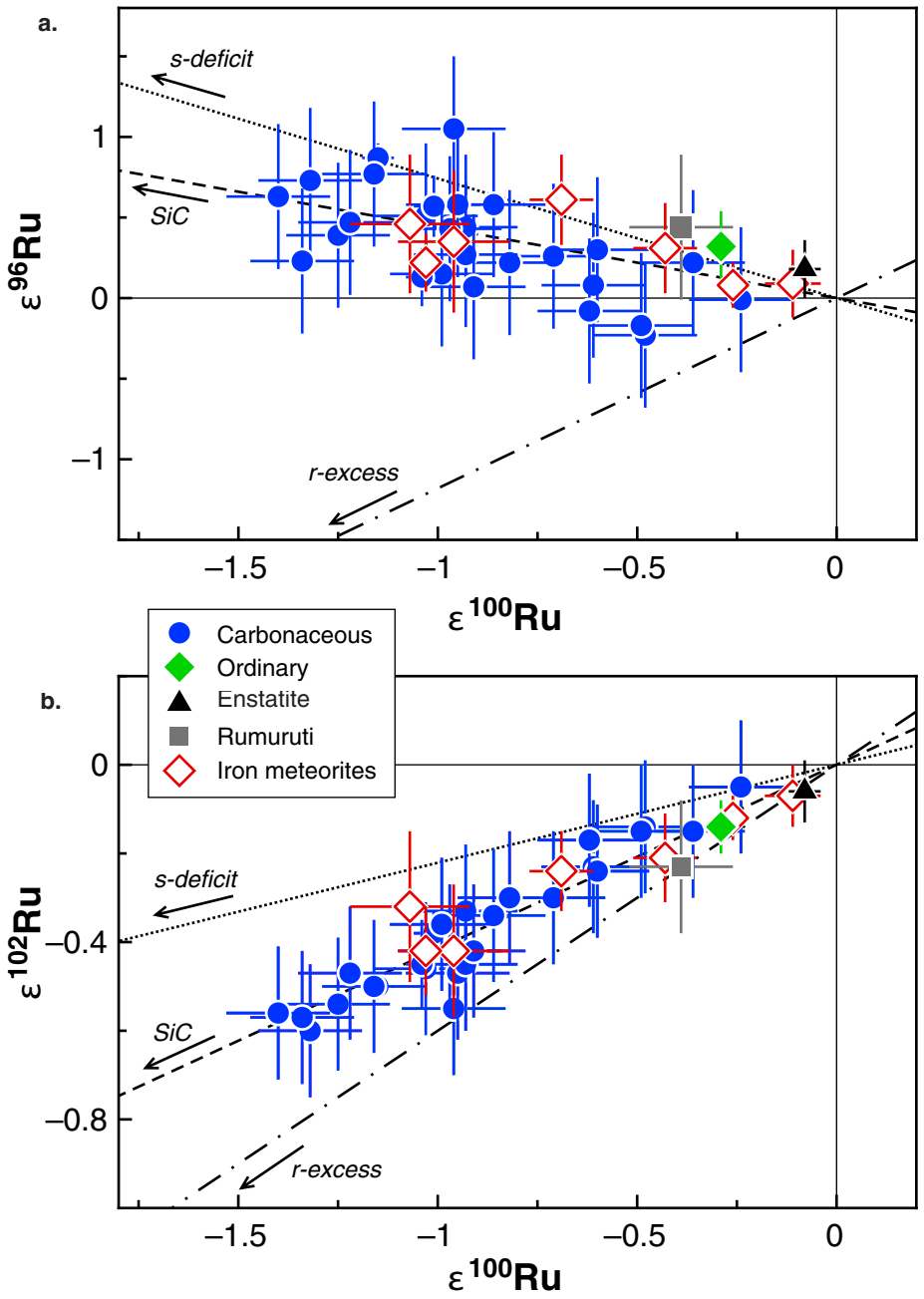

Extended Data Figure 1 | Ruthenium isotope plots for chondrites and iron meteorites. a, ε^{100}Ru–ε^{96}Ru; **b**, ε^{100}Ru–ε^{102}Ru. See the source data for Extended Data Fig. 1. Lines represent mixing lines between terrestrial Ru and an *s*-process component as defined by Ru isotope data for presolar SiC[32] (dashed line), calculated *s*-process yields[33] (dotted line) and corresponding calculated residuals for rapid neutron capture process (r-process) of stellar nucleosynthesis (dashed-dotted line). Uncertainties of individual data points reflect the external uncertainty of the method (2 s.d., for samples measured $n < 4$ times) or 95% confidence intervals (calculated as two-sided Student's *t*-values, for samples measured $n \geq 4$ times). Uncertainties for group averages of ordinary and enstatite chondrites are 95% confidence intervals, and uncertainties for non-magmatic IAB iron meteorites include propagated errors from secondary neutron-capture correction as given in Extended Data Table 2. Data for other iron meteorites are from ref. 11.

Extended Data Table 1 | Ruthenium isotope data of chondrites and terrestrial chromitites

Sample	Group	$\varepsilon^{96}Ru^*$	$\varepsilon^{98}Ru^*$	$\varepsilon^{100}Ru^*$	$\varepsilon^{102}Ru^*$	$\varepsilon^{104}Ru^*$
Carbonaceous chondrites						
Orgueil	CI	-0.01 ± 0.45	0.08 ± 0.52	-0.24 ± 0.13	-0.05 ± 0.15	0.07 ± 0.31
Tagish Lake	C2-ung	0.51 ± 0.45	-0.26 ± 0.52	-1.03 ± 0.13	-0.46 ± 0.15	-0.02 ± 0.31
Murchison	CM2	-0.23 ± 0.45	-0.47 ± 0.52	-0.48 ± 0.13	-0.14 ± 0.15	0.06 ± 0.31
Murchison†	CM2	0.44 ± 0.45	0.51 ± 0.52	-0.93 ± 0.13	-0.33 ± 0.15	0.11 ± 0.31
Ibilit Winselvan	CM2	0.58 ± 0.45	0.08 ± 0.52	-0.86 ± 0.13	-0.34 ± 0.15	0.14 ± 0.31
LON 94101	CM2	-0.17 ± 0.45	-0.48 ± 0.52	-0.49 ± 0.13	-0.15 ± 0.15	0.08 ± 0.31
NWA 801	CR2	0.26 ± 0.45	0.46 ± 0.52	-0.71 ± 0.13	-0.30 ± 0.15	0.15 ± 0.31
NWA 1180	CR2	0.08 ± 0.45	0.08 ± 0.52	-0.61 ± 0.13	-0.23 ± 0.15	0.13 ± 0.31
GRA 06100	CR2	1.05 ± 0.45	-0.11 ± 0.52	-0.96 ± 0.13	-0.55 ± 0.15	0.04 ± 0.31
Tafassasset metal†	CR-an	0.87 ± 0.09	0.38 ± 0.19	-1.15 ± 0.04	-0.50 ± 0.03	0.16 ± 0.09
NWA 2090	CO3	0.22 ± 0.45	0.37 ± 0.52	-0.36 ± 0.13	-0.15 ± 0.15	0.09 ± 0.31
Kainsaz	CO3	0.77 ± 0.45	0.37 ± 0.52	-1.16 ± 0.13	-0.50 ± 0.15	0.05 ± 0.31
NWA 5933	CO3	0.39 ± 0.45	0.44 ± 0.52	-1.25 ± 0.13	-0.54 ± 0.15	-0.11 ± 0.31
Maralinga	CK4-an	0.43 ± 0.45	0.25 ± 0.52	-0.97 ± 0.13	-0.42 ± 0.15	0.09 ± 0.31
NWA 6604	CK4	0.58 ± 0.45	0.37 ± 0.52	-0.95 ± 0.13	-0.47 ± 0.15	0.04 ± 0.31
NWA 4679	CK4	0.22 ± 0.45	-0.17 ± 0.52	-0.82 ± 0.13	-0.30 ± 0.15	0.11 ± 0.31
NWA 6009	CK6	0.47 ± 0.45	0.31 ± 0.52	-1.22 ± 0.13	-0.47 ± 0.15	0.25 ± 0.31
DaG 412	CK5	0.73 ± 0.45	0.91 ± 0.52	-1.32 ± 0.13	-0.60 ± 0.15	0.07 ± 0.31
DaG 250	CK4/5	0.23 ± 0.45	0.15 ± 0.52	-1.34 ± 0.13	-0.57 ± 0.15	0.10 ± 0.31
Allende MSA†,‡	CV3	0.57 ± 0.19	0.52 ± 0.21	-1.01 ± 0.05	-0.38 ± 0.05	0.19 ± 0.10
Allende B	CV3	0.30 ± 0.45	0.15 ± 0.52	-0.60 ± 0.13	-0.24 ± 0.15	0.15 ± 0.31
NWA 6717	CV3	0.27 ± 0.45	0.30 ± 0.52	-0.93 ± 0.13	-0.45 ± 0.15	-0.05 ± 0.31
NWA 8333	CV3	0.63 ± 0.45	0.64 ± 0.52	-1.40 ± 0.13	-0.56 ± 0.15	0.11 ± 0.31
Vigarano	CV3	0.15 ± 0.45	0.17 ± 0.52	-0.99 ± 0.13	-0.36 ± 0.15	0.15 ± 0.31
Efremovka	CV3	-0.08 ± 0.45	0.22 ± 0.52	-0.62 ± 0.13	-0.17 ± 0.15	0.21 ± 0.31
Acfer 214	CH	0.07 ± 0.45	-0.33 ± 0.52	-0.91 ± 0.13	-0.42 ± 0.15	-0.10 ± 0.31
Gujba metal†	CB	0.13 ± 0.18	0.26 ± 0.29	-1.04 ± 0.04	-0.45 ± 0.10	-0.08 ± 0.20
Rumuruti chondrites						
NWA 753	R3.9	0.44 ± 0.45	0.90 ± 0.52	-0.39 ± 0.13	-0.23 ± 0.15	-0.21 ± 0.31
Ordinary chondrites						
Kunashak	L6	0.06 ± 0.45	0.17 ± 0.52	-0.28 ± 0.13	-0.16 ± 0.15	-0.03 ± 0.31
Ochansk†	H4	0.66 ± 0.45	0.41 ± 0.52	-0.30 ± 0.13	-0.22 ± 0.15	-0.20 ± 0.31
Bath†	H4	0.47 ± 0.45	-0.15 ± 0.52	-0.32 ± 0.13	-0.07 ± 0.15	0.30 ± 0.31
Monroe†	H4	0.21 ± 0.45	0.17 ± 0.52	-0.26 ± 0.13	-0.11 ± 0.15	0.19 ± 0.31
Forest Vale†	H4	0.25 ± 0.45	0.42 ± 0.52	-0.26 ± 0.13	-0.11 ± 0.15	0.06 ± 0.31
Pantar†	H5	0.28 ± 0.45	0.24 ± 0.52	-0.32 ± 0.13	-0.15 ± 0.15	-0.05 ± 0.31
	Mean§	0.32 ± 0.22	0.21 ± 0.22	-0.29 ± 0.03	-0.14 ± 0.06	0.04 ± 0.19
Enstatite chondrites						
PCA 91020	EL3	-0.10 ± 0.45	0.04 ± 0.52	0.02 ± 0.13	-0.02 ± 0.15	0.08 ± 0.31
TIL 91714	EL5	0.09 ± 0.45	-0.05 ± 0.52	-0.10 ± 0.13	-0.02 ± 0.15	0.03 ± 0.31
Daniel's Kuil†	EL6	0.21 ± 0.45	0.47 ± 0.52	-0.16 ± 0.13	-0.21 ± 0.15	-0.01 ± 0.31
Khairpur†	EL6	0.17 ± 0.45	0.02 ± 0.52	-0.08 ± 0.13	-0.03 ± 0.15	0.16 ± 0.31
ALHA 81021	EL6	0.01 ± 0.45	-0.33 ± 0.52	-0.06 ± 0.13	-0.02 ± 0.15	0.03 ± 0.31
LAP 10130	EL6	0.30 ± 0.45	0.15 ± 0.52	-0.09 ± 0.13	-0.15 ± 0.15	-0.13 ± 0.31
GRO 95517	EH3	0.52 ± 0.45	0.05 ± 0.52	-0.10 ± 0.13	-0.05 ± 0.15	0.00 ± 0.31
LAR 06252	EH3	-0.07 ± 0.45	0.04 ± 0.52	-0.06 ± 0.13	0.11 ± 0.15	0.37 ± 0.31
Abee	EH4	0.52 ± 0.45	0.56 ± 0.52	-0.09 ± 0.13	-0.12 ± 0.15	-0.08 ± 0.31
	Mean§	0.18 ± 0.18	0.10 ± 0.21	-0.08 ± 0.04	-0.06 ± 0.07	0.05 ± 0.11
Terrestrial chromitites						
Shetland (C3)†		-0.04 ± 0.11	0.01 ± 0.19	0.04 ± 0.06	0.01 ± 0.09	-0.05 ± 0.22
Bushveld (UG2)		0.14 ± 0.24	0.24 ± 0.49	0.05 ± 0.09	-0.11 ± 0.14	-0.24 ± 0.22

*Ruthenium isotope data are internally normalized to $^{99}Ru/^{101}Ru$ using the exponential law and are reported as ε-unit (0.01%) deviations from the terrestrial bracketing standard: $\varepsilon^iRu = (^iRu/^{101}Ru_{sample}/^iRu/^{101}Ru_{standard} - 1) \times 10^4$, where $i = 96, 98, 100, 102$ or 104. For samples measured $n < 4$ times quoted errors reflect the external uncertainty as defined by the standard deviation (2 s.d.) of repeated analysis of reference samples (see Methods). Uncertainties for samples analysed $n \geq 4$ times are given as 95% confidence intervals of the mean calculated as: (s.d. $\times t_{0.95, n-1}$)/$\sqrt{n}$.

†Data previously reported[11].

‡Average data calculated from replicate alkaline fusion digestions[11].

§Calculated group averages with 95% confidence interval uncertainties calculated as: (s.d. $\times t_{0.95, n-1}$)/$\sqrt{n}$.

Extended Data Table 2 | Measured Ru and Pt isotope data and neutron-capture-corrected ε^{i}Ru values for non-magmatic iron meteorites (group IAB)

a

Sample	class	ε^{96}Ru*	ε^{98}Ru*	ε^{100}Ru*	ε^{102}Ru*	ε^{104}Ru*	ε^{196}Pt†
Campo del Cielo	IAB	0.26 ± 0.16	0.41 ± 0.19	0.01 ± 0.05	0.01 ± 0.06	0.19 ± 0.15	0.20 ± 0.07
Landes	IAB	0.35 ± 0.20	0.15 ± 0.66	-0.08 ± 0.08	-0.01 ± 0.05	0.17 ± 0.17	0.05 ± 0.07
Nantan	IAB	0.15 ± 0.18	0.12 ± 0.34	-0.06 ± 0.02	-0.02 ± 0.06	0.15 ± 0.19	0.08 ± 0.07
Canyon Diablo	IAB	0.22 ± 0.16	0.33 ± 0.29	0.05 ± 0.04	0.06 ± 0.03	0.08 ± 0.08	0.30 ± 0.07

b

	ε^{96}Ru	ε^{98}Ru	ε^{100}Ru	ε^{102}Ru	ε^{104}Ru
$IAB_{pre\text{-}exp.}$	0.09 ± 0.21	0.17 ± 0.39	-0.11 ± 0.07	-0.07 ± 0.07	-0.04 ± 0.19

a, Measured ε^{i}Ru and ε^{196}Pt values. **b**, Neutron-capture-corrected (pre-exposure) ε^{i}Ru values. Average $IAB_{pre\text{-}exposure}$ ε^{i}Ru values were calculated from measured ε^{i}Ru and ε^{196}Pt data of individual IAB samples as given in **a**, corrected for neutron-capture-induced isotope shifts using the equation $\varepsilon^{i}Ru_{pre\text{-}exposure} = \varepsilon^{i}Ru_{measured} - \varepsilon^{196}Pt \times slope$, where the slope was obtained from linear regression calculation of empirical correlations of ε^{196}Pt with ε^{i}Ru for IIAB iron meteorites[11] (slopes ε^{196}Pt–ε^{96}Ru: 0.98 ± 0.53; ε^{196}Pt–ε^{98}Ru: 0.17 ± 0.40; ε^{196}Pt–ε^{100}Ru: 0.55 ± 0.16; ε^{196}Pt–ε^{102}Ru: 0.52 ± 0.18; ε^{196}Pt–ε^{104}Ru: 1.2 ± 0.4). Quoted uncertainties reflect propagated errors, including uncertainties on ε^{i}Ru, ε^{196}Pt and ε^{196}Pt–ε^{i}Ru slopes.

*See the footnote to Extended Data Table 1 for explanation. Quoted uncertainties represent 95% confidence intervals for replicate analyses ($n \geq 4$) of the same sample solutions, calculated as: $(\text{s.d.} \times t_{0.95,\, n-1})/\sqrt{n}$.

†Platinum isotope data were measured on the same sample digestion solution used for Ru. The analytical procedure for Pt isotope analyses is as outlined elsewhere (ref. 34).